Journal Pre-proof

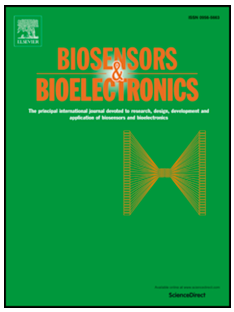

Cancer cell detection device for the diagnosis of bladder cancer from urine

Melanie MacGregor, Hanieh Safizadeh Shirazi, Kit Man Chan, Kola Ostrikov, Kym McNicholas, Alex Jay, Michael Chong, Alexander H. Staudacher, Thomas D. Michl, Aigerim Zhalgasbaikyzy, Michael P. Brown, Moein Navvab Kashani, Adam Di Fiore, Alex Grochowski, Stephen Robb, Simon Belcher, Jordan Li, Jonathan M. Gleadle, Krasimir Vasilev

PII: S0956-5663(20)30688-6

DOI: https://doi.org/10.1016/j.bios.2020.112699

Reference: BIOS 112699

To appear in: *Biosensors and Bioelectronics*

Received Date: 2 October 2020

Accepted Date: 5 October 2020

Please cite this article as: MacGregor, M., Shirazi, H.S., Chan, K.M., Ostrikov, K., McNicholas, K., Jay, A., Chong, M., Staudacher, A.H., Michl, T.D., Zhalgasbaikyzy, A., Brown, M.P., Kashani, M.N., Di Fiore, A., Grochowski, A., Robb, S., Belcher, S., Li, J., Gleadle, J.M., Vasilev, K., Cancer cell detection device for the diagnosis of bladder cancer from urine, *Biosensors and Bioelectronics* (2020), doi: https://doi.org/10.1016/j.bios.2020.112699.

Cancer cell detection device for the diagnosis of bladder cancer from urine.

Melanie MacGregor‡[a]*, Hanieh Safizadeh Shirazi‡[a,b], Kit Man Chan[b], Kola Ostrikov[a,b], Kym McNicholas[c,d], Alex Jay[d,e], Michael Chong[d,e], Alexander H. Staudacher[f,g], Thomas D. Michl[b], Aigerim Zhalgasbaikyzy[b], Michael P. Brown[f,g,h], Moein Navvab Kashani[a,i], Adam Di Fiore[j], Alex Grochowski[j], Stephen Robb[j], Simon Belcher[j], Jordan Li[c,d], Jonathan M. Gleadle[c,d], Krasimir Vasilev[a,b].

[a] Future Industry Institute, University of South Australia, Mawson Lakes, SA, Australia 5095

[b] School of Engineering, University of South Australia, Mawson Lakes, SA, Australia 5095

[c] Department of Renal Medicine, Flinders Medical Centre, Bedford Park, SA, Australia, 5042

[d] College of Medicine and Public Health, Flinders University, Bedford Park, SA, Australia, 5042

[e] Department of Urology, Flinders Medical Centre, Bedford Park, SA, Australia, 5042

[f] Translational Oncology Laboratory, Centre for Cancer Biology, SA Pathology and University of South Australia, Adelaide, SA, Australia 5000

[g] School of Medicine, University of Adelaide, SA, Adelaide, Australia 5000

[h] Cancer Clinical Trials Unit, Royal Adelaide Hospital, SA, Adelaide, Australia 5000

[i] South Australian Node of the Australian National Fabrication Facility, University of South Australia, Mawson Lakes, SA, Australia 5095

[j] Motherson Innovations Australia, Lonsdale, SA, Australia 5160.

*Corresponding Author: UniSA Mawson lakes campus, MM building, Mawson lakes Bvd, Mawson Lakes, SA 5095, Australia; Melanie.Macgregor@unisa.edu.au

ABSTRACT Bladder cancer is common and has one of the highest recurrence rates. Cystoscopy, the current gold standard diagnosis approach, has recently benefited from the introduction of blue light assisted photodynamic diagnostic (PDD). While blue light cystoscopy improves diagnostic sensitivity, it remains a costly and invasive approach. Here, we present a microfluidic-based platform for non-

invasive diagnosis which combines the principle of PDD with whole cell immunocapture technology to detect bladder cancer cells shed in patient urine *ex vivo*. Initially, we demonstrate with model cell lines that our non-invasive approach achieves highly specific capture rates of bladder cancer cells based on their Epithelial Cell Adhesion Molecule expression (>90%) and detection by the intensity levels of Hexaminolevulinic Acid-induced Protoporphyrin IX fluorescence. Then, we show in a pilot study that the biosensor platform successfully discriminates histopathologically diagnosed cancer patients (n=10) from non-cancer controls (n=25). Our platform can support the development of a novel non-invasive diagnostic device for post treatment surveillance in patients with bladder cancer and cancer detection in patients with suspected bladder cancer.

***KEYWORDS**: Bladder cancer; cystoscopy; Hexaminolevulinic Acid; immunocapture; photodynamic diagnosis; EpCAM; biosensor; microfluidic device; plasma deposition; PpIX fluorescence; biofluids*

1. Introduction

Bladder cancer is amongst the 10 most common cancers in developed countries, ranking as high as 4th for men in the U.S.(Jordan and Meeks, 2019). Of all cancers, bladder cancer is the most expensive to treat from diagnosis to death (Sievert et al., 2009) because of its particularly high recurrence rate of up to 80% in high-grade tumours (Jung et al., 2019). Current guidelines recommend that patients with an intermediate-risk of recurrence undergo cystoscopic surveillance every 3-6 months for 2 years, and at least yearly thereafter (Babjuk et al., 2017). The gold standard for initial diagnosis and follow-up is white light cystoscopy (WLC) followed by biopsy and histopathology, if there are suspicious lesions (Bell et al., 2016). This approach is invasive, and its accuracy relies on the macroscopic visibility of the malignant lesions being biopsied (Dinney et al., 2004). Due to the invasive nature of the procedure, patients need to be hospitalised and may experience complications such as infections and bleeding (Biardeau et al., 2017). Over the last decade, fluorescence-assisted cystoscopy has emerged as a valid

procedure to further improve the detection and resection of bladder cancer; compared to WLC alone (Witjes and Douglass, 2007). Referred to as photodynamic diagnosis, blue light cystoscopy (BLC) exploits the photoactive properties of Protoporphyrin IX (PpIX) to enhance the contrast between benign and malignant tissue during cystoscopic examination (Geavlete et al., 2016). The exogenous administration of hexaminolevulinate (HAL) leads to the preferential accumulation of fluorescent PpIX in rapidly proliferating cells, such as those in cancerous tissues. This accumulation leads to a distinctive red fluorescence (maximum emission at 635 nm) when illuminated with blue-violet light (maximum adsorption at 405 nm) (McNicholas et al., 2019; Schmidbauer et al., 2004). Since its FDA approval in 2010, extensive data have shown that BLC improves bladder cancer detection rates. In comparison to BLC, the reported sensitivity of WLC ranges from 46 to 84% and its specificity from 31 to 93% (Witjes and Douglass, 2007). BLC performs particularly well for low-grade tumours detection, which translates to a decrease in recurrence rates (Gallagher et al., 2017; Lotan et al., 2019). Now recommended in several urological guidelines around the world, BLC constitutes a significant breakthrough in bladder cancer diagnosis. Yet, BLC remains just as invasive and more costly and time consuming than WLC alone. The reason being that HAL requires instillation 60 minutes prior to cystoscopy, a specialized camera and an adapter for cystoscopy.

There is a clear need for less invasive methods for bladder cancer detection and surveillance. Although non-invasive diagnostic approaches based on urinary biomarker detection have been developed, none has been adopted into widespread clinical practice due to insufficient sensitivity and specificity rates compared to WLC (Bubendorf et al., 2016). To date, only urine cytology is a standard non-invasive test in the clinical setting. Although the cellularity of healthy urine is low, it is well-documented that bladder cancer cells are shed in the urine of cancer patients (Khoo et al., 2019; Kiyoshima et al., 2016; McGrew, 1961). Cytologic examination of urine specimens for exfoliated bladder cancer cells has high sensitivity in high grade bladder cancer (84%) (Lotan and Roehrborn, 2003; Planz et al., 2005). Howev-

er, it has much lower sensitivity in low grade bladder cancer (16%) (Yafi et al., 2015), thus limiting the usefulness of urine cytology as a diagnostic test for bladder cancer (Yafi et al., 2014). In addition, the specificity of urine cytology is variable (Barkan et al., 2016) and can be influenced by common conditions like urinary tract infection, stone disease or previous instillation of either intravesical chemotherapy or Bacillus Calmette Guerin (BCG) all of which occur frequently in this population. The resulting extracellularity of the urine samples tend to obstruct the cytologist field of view with cells that often have similar cytomorphology as cancer cells, making them hard to distinguish. For these reasons, urine cytology is used mainly as an adjunct in managing patients with known high-grade diseases.

Interestingly, recent developments in non-invasive methods to detect bladder cancer from urine have not attempted to solve the issues faced by classic cytology. Instead, most research has taken the direction to focus on the detection of soluble proteins biomarkers, such as complement factor H-related protein and nuclear matrix protein, (Chakraborty, Ashish et al., 2019) or new omics biomarkers (Frantzi et al., 2016; Shen et al., 2015) in tests that typically detect DNA methylation, mutation or mRNA expression using PCR, SAGE and/or mass spectrometry methods. (Chakraborty, A. et al., 2019; Dinges et al., 2019; Tan et al., 2018) While these tests generally have higher sensitivity than urine cytology, they have the disadvantage of relying on expensive reagents and complex analytical platforms and their overall accuracy has not been sufficient to justify changes in diagnostic or surveillance protocols, as we recently reviewed in details.(Chan, 2020).

In contrast, inspired by recent developments in the field of circulating tumor cell capture from blood, (Arya et al., 2013) we demonstrated in previous works, that a immunofunctionalised microfluidic chip could be use to capture and concentrate cancer cells spiked in urine, thus overcoming the issue of extracellularity and cytomorphology limitations faced by classic urine cytology.(Macgregor-Ramiasa et al., 2017a) While promising, this immune-capture approach alone could not be used as a point of care diag-

nostic tool because it lacked the specific signal needed for the automation of the malignant cells detection step from the captured cell population. It is this last roadblock that we propose to resolve here, using the photodynamic principle of blue light cystoscopy but applied ex-vivo at the single cell level, in order to keep the whole approach non invasive. Fujimoto's group has demonstrated that 5ALA could be used to assist cytological examination in the sediment of urine samples processed following the same steps as classic cytology, and using spectrophotometers to evaluate the overall fluorescence of the whole specimen. (Nakai et al., 2015), (Nakai et al., 2017). However, for this approach to be viable as a building block for novel point of care diagnostic device, two key challenges need to be overcome using unprocessed patient urine samples. First, whole cancer cells shed by the tumors must be successfully isolated from unprocessed urine samples. Second, individual cell must be distinguishable from other cell type based on their PpIX fluorescence

The goal of this study is to develop a non-invasive bladder cancer diagnostic device which could serve as an alternative for WLC and BLC in clinical contexts such as routine surveillance post tumour resection. We hypothesise that bladder cancer cells excreted in the urine of patients can be selectively captured via immunoaffinity on a purposely designed microfluidic platform and detected *ex situ* using the photodynamic properties of HAL. To achieve this, we have covalently immobilised bioactive anti-epithelial cell adhesion molecule (EpCAM) antibodies to the surface of microchannels (Ostrikov et al., 2019). The biofunctionalization of the surface was achieved via facile "click-type" chemistry of the EpCAM antibodies to a thin oxazoline plasma polymer (Macgregor-Ramiasa et al., 2017b; Macgregor-Ramiasa et al., 2015; Shirazi et al., 2020). These antibody decorated surfaces enable the selective immunocapture of bladder cancer cells; which are known to have greater expression of the EpCAM protein on their membranes compared to other cells present in urine. The selective immunocapture ap-

proach employed in this endeavour is much less problematic in urine than in blood (Zhe et al., 2011) because it takes unique advantage of the upstream filtration work performed by the kidneys which excludes circulating blood cells. The diagnostic method developed in this work uniquely takes advantage of HAL induced cancer-specific PpIX fluorescence in the malignant cells isolated in the microfluidic chamber for quantification. Because of this distinctive combination of technologies, we called the method Microfluidic Urinary Photo-Specific Diagnostic of bladder cancer, simply abbreviated as MicroUPSD (**Fig. 1**). It was optimised to achieve high sensitivity and efficiency. These qualities were first verified using model cell lines spiked into both PBS and patient urine samples. The refined diagnostic method was then verified with patient's urine specimens.

2. Materials and Methods

The study design and working principle of the diagnostic approach are summarised in **Fig. 1**.

2.1 Sensor design via Oxazoline plasma polymerization

The plastic moulded fluidic chamber (PMFC, Motherson Innovations Australia) consists of a flat lid with 3 sets of inlets and outlets bound to a bottom plate featuring 3 channel grooves using an adhesive

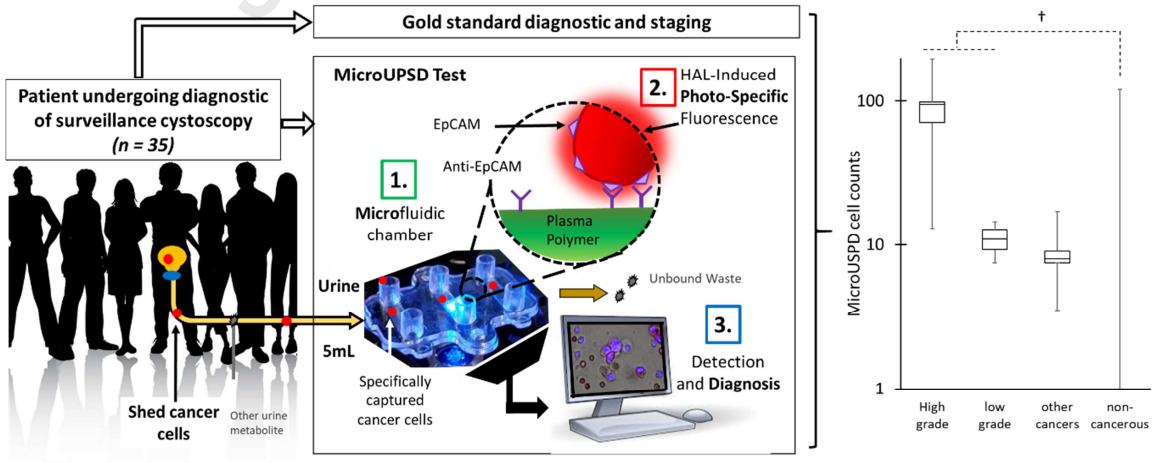

layer.

Figure 1. Schematic of the Microfluidic Urinary Photo-Specific Diagnostic (MicroUPSD) device working principle and study design. First, patient urine is treated with the photosensitizer prodrug HAL and a nuclear stain (NucRed).Then it is passed through the specially designed microfluidic chamber functionalised with anti-EpCAM antibodies, a membrane biomarker specific for cancer cells.(Bryan et al., 2014) . After a set incubation time, the capture channels are rinsed with PBS to dislodge cells that are not bound to the active surface and fluorescent micrographs are recorded. The latter are then analysed for colocalised nuclear and HAL-induced fluorescence in the captured cell population. The nuclear stain is used to confirm that the HAL positive events recorded are indeed cells and not debris or artefacts. The box plot results on the right show the results as glance for high- and low-grade bladder cancer, as well as other urogenital cancers (prostate) and non-cancerous participants. (†=$p<0.1$).

The capture channels are designed to provide a laminar fluid flow around surface-bound cells upon rinsing (**Fig. 2A** and **SupVid. 1**). Each micro channel has a total capacity of 45µL (18L x 3.8W x 0.53H mm) from which 24 µL fill the imaging zone between the channel wells, where the cells are counted. A custom-built capacitively coupled bell-chamber reactor was used to deposit a thin layer of 2-methyl-2-oxazoline (POx) precursor onto the PMFC. The plasma was ignited for 3 minutes using a radio frequency power of 50 W (13.5 MHz) and a monomer pressure of $1.3.10^{-1}$ mbar (Cavallaro et al., 2016; MacGregor-Ramiasa et al., 2016; Macgregor-Ramiasa et al., 2015). The POx coating in the test microchannel was functionalized using Anti-Epithelial Cell Adhesion molecule antibodies (Anti-EpCAM, 10 µg/mL) by overnight incubation at 4 °C followed by 1 hour at 37 ^{o}C the next day. A blocking solution, (e.g. skim milk, 1mg/mL) was then added to the channel with Anti-EpCAM and one of the other microchannels for 1h incubation. This second blocked microchannel is used as negative control. After incuba-

tion, the block was rinsed from both channels using 600 µL PBS. PBS was added to all 3 channels and kept at room temperature for no longer than 1h before testing.

2.2 Cell line study

Human foreskin fibroblast (HFF) were cultured in Dulbecco's Modified Eagles Medium (DMEM). Four bladder cancer cell lines were supplied by the European Collection of Cell Cultures (ECACC; Salisbury, United Kingdom) and purchased from CellBank Australia (NSW, Australia). RT4 (Cat No: 91091914) was cultured in McCoy's 5A medium, EJ138 (Cat No: 85061108), HT1376 (Cat No: 87032402) and HT1197 (Cat No: 87032403) were cultured in Minimum Essential Medium Eagle (MEME) with 1% MEM Non-essential Amino Acid Solution (MEM-NEAA). All cultures were supplemented with 10% fetal bovine serum (FBS), 2 mM L-glutamine, 5% penicillin-streptomycin (pen-strep) and 5% amphotericin B solution. All cell lines were grown at 37 °C in 5% CO_2 in a humidified atmosphere. Phosphate-buffered saline (PBS) tablets, DMEM, pen-strep (10,000 U/mL), L-glutamine (200 mM) and FBS were purchased from Life Technologies (VIC, Australia). Amphotericin B solution, MEME, McCoy's 5A medium, MEM-NEAA and fungizone were obtained from Sigma-Aldrich (NSW, Australia).

Flow Cytometry, Immunocytochemistry, Western Blot were performed to investigate EpCAM expression in Fibroblasts, RT4, HT-1197, HT-1376 and EJ138 cell lines following established procedures, as detailed in supplementary information.

2.3 HAL Optimization

Hexaminolevulinate (HAL) hydrochloride was obtained from Sigma-Aldrich (NSW, Australia) and PBS was used make solutions with concentration ranging 0 to 250 µM. Cells were seeded in a 96 well plate (Corning, NY) at 37°C in 5% CO_2 overnight. All cells monolayers were then incubated in their

own serum-free medium containing different concentrations of HAL (0-250 µM) at 37°C in the dark for 30 min to 4 h. After HAL incubation, the HAL containing medium was removed and replaced by PBS. The plates imaged with an Olympus IX83 inverted fluorescent microscope (Japan) (excitation wavelength: 405nm, emission wavelength: 600nm with a custom filter cube). To determine the PpIX fluorescence intensities, region of interests (ROI) were defined for 30 randomly selected cells in each image and the values of the average gray intensity for each of these objects were calculated using CellSens software (Olympus, Japan). Each HAL incubation condition was repeated in biological triplicates.

To test trypsinized cells in suspension, the cells were resuspended in serum-free medium and were treated with HAL as described above. After incubation, the cells were centrifuged at 1500 rpm for 5 min and the supernatant discarded. The cells were resuspended in PBS and transferred to a 96-well plate. The plate was read using a specially designed fluorescent microscope with appropriate LED lamps and custom filters (Chan et al., 2019). PpIX accumulation was observed in the images and the fluorescence intensity was measured using ImagePro Premier software (USA). ImagePro in-build cell counting algorithm uses auto-thresholding to automatically detect and calculate the average fluorescence intensity of all the cells present in each image. Each HAL incubation condition was repeated in triplicates.

2.4 Capture Experiment

The selectivity of the cell capture approach was tested with different anti-EpCAM antibodies (AF960, Invitro Life Science; VU-1D9, Biosensis and ABCAM; MOC-31, ABCAM Australia; BER-EP4 ,ABCAM Australia; HPA ,Sigma-Aldrich; 22-HCLC, Thermo Scientific Australia) Cultured cells were collected and resuspended in PBS. Bladder cancer cells were stained with 0.5 µM Nuclear-Red and normal fibroblast HFF cells were stained with NucBlue Live Cell Stain Ready Probes reagent (Life technologies) following the manufacturer's instructions. Both cell types were stained for 15 minutes at 37°C. The cells were then pelleted and washed twice with PBS prior to injection in the microfluidic

channels. The cells were left to interact with the capture substrates for 45 minutes before rinsing with 1 mL of PBS. All experiments were done in triplicates, from which the averages and standard deviations were obtained.

2.5 Pilot clinical study

For the pilot clinical study, urine specimens were prospectively collected from 51 patients admitted for cystoscopy under the care of the Urology Department, Flinders Medical Centre in accordance with the protocol approved by the Southern Adelaide Clinical Human Research Ethics Committee (HREC/15/SAC/478 485.15). The optimisation cohort consisted of 16 patients. 5 patients had confirmed bladder cancer and 3 patients had renal cell carcinoma. 8 patients had non-cancerous conditions and/or normal cystoscopy examination. The validation cohort consisted of 35 patients; 6 patients had histopathologically confirmed bladder cancer, 3 patients had prostate cancer and 1 patient had bowl cancer that had invaded the bladder wall. 25 control patients had non-cancer conditions and/or normal cystoscopic examination. Each patient provided written consent prior to the collection of the urine sample for this proof of concept feasibility study**. Sup Table 2 and 3** provide patient information.

30-50 mL of voided urine was collected from the participants. After collection, the specimens were kept at 4^{o}C until further processing which occurred within 6 h post collection. Once received, the samples were agitated gently to resuspend any settled material and were processed in two ways, namely settling (SET) and centrifuging (CU). In the SET protocol, 2.5 ml of urine was transferred to a 15 mL tube and diluted with 2.5 ml of PBS. HAL (50 μM) was added to the mixture and kept in the dark for 1-2 hour to settle without any disturbing (Chan et al., 2019). 300 μL of the settled urine was then collected and 0.5 μM Nuclear-Red added. The Nuclear Red dye was used to discriminate between actual cells and other artefacts such as debris. In the CU procedure, 5 mL of urine was transferred to a falcon tube. 50 μM of HAL was added to it and kept in the dark. After 1-2 h incubation, the patient sample was centri-

fuged at 1500 rpm for 5 min. After centrifugation, a 300 µL pellet of the 5 mL of centrifuged urine was collected and 0.5 µM Nuclear-Red added. After both settling and centrifuging, the test sensor microchannels were loaded with the stained urine sample (3 channels for block, POx and EpCAM, each filled with 45 µL of urine concentrate) and imaged with a fluorescence microscope. Each patient sample was processed in duplicates.

The images were analysed using Image-Pro software. As a first selection criterion, the software excluded objects with diameter outside of the range 7 to 53 µm. Second, the remaining objects that displayed co-localised HAL-induced fluorescence and Nuclear Red signal were manually counted as cells. Absolute numbers of Nuclear Red and HAL-positive cells captured in the EpCAM and Block microchannels were recorded. The Block channel is a negative control to identify the level of non-specific cell binding to the surface. The number of cells bound in the block channel and were counted and deducted from the cell numbers in the EpCAM channel. As a third criterion, the test was deemed positive if the number of positive cells bound to the EpCAM channel was higher than in the block channel. The Sensitivity, Specificity, Positive Predictive Value (PPV), and Negative Predictive Value (NPV) were calculated using standard equations, as detailed in supplementary information.

3. Results

Diagnostic Device design. The technology that forms the basis of the device used in this study is a polyoxazoline-based plasma polymer coating (POx) that we designed (Ramiasa et al., 2015; Vasilev et al., 2015). Plasma deposition is a versatile, solvent free and substrate independent technique which enables the deposition of thin functional films within minutes. The POx coatings plasma deposited from the plasma phase of 2-methyl-oxazoline (**Fig. 2B**) are 50 nm thick, smooth, hydrophilic and stable in a range of physiologically relevant fluids, including urine (**SupFig. 1**) (Vasilev et al., 2017). The coatings consists of chemical groups containing carbon, oxygen and nitrogen. Most importantly, the outermost

surface is rich in intact oxazoline rings, as demonstrated by several independent research groups, (Macgregor et al., 2017; Zanini et al., 2016) (**SupFig. 1**). The latter enable the irreversible binding of bioactive antibodies via a spontaneous "click-type" reaction occurring in PBS between the oxazoline ring and carboxylic acid group present in the biomolecule; as previously shown via ToF-SIMS principal component analysis (Macgregor-Ramiasa et al., 2017b; Macgregor-Ramiasa et al., 2015). The microfluidic device features three separated chambers to provide one positive control channel, one negative control and one test channel. All three chambers were coated with POx. In the first chamber, the unaltered POx surface was used as a positive control because it non-specifically binds all cell types. In the test channel, the unique reactivity of the POx surface was used to functionalise the channel with anti-EpCAM antibody. A block solution was added in a follow-up step to block the underlying reactive POx substrate and limit non-specific adhesion. The last channel was blocked with the same blocking solution alone and used as negative control, offering little to no adhesion for any cell type.

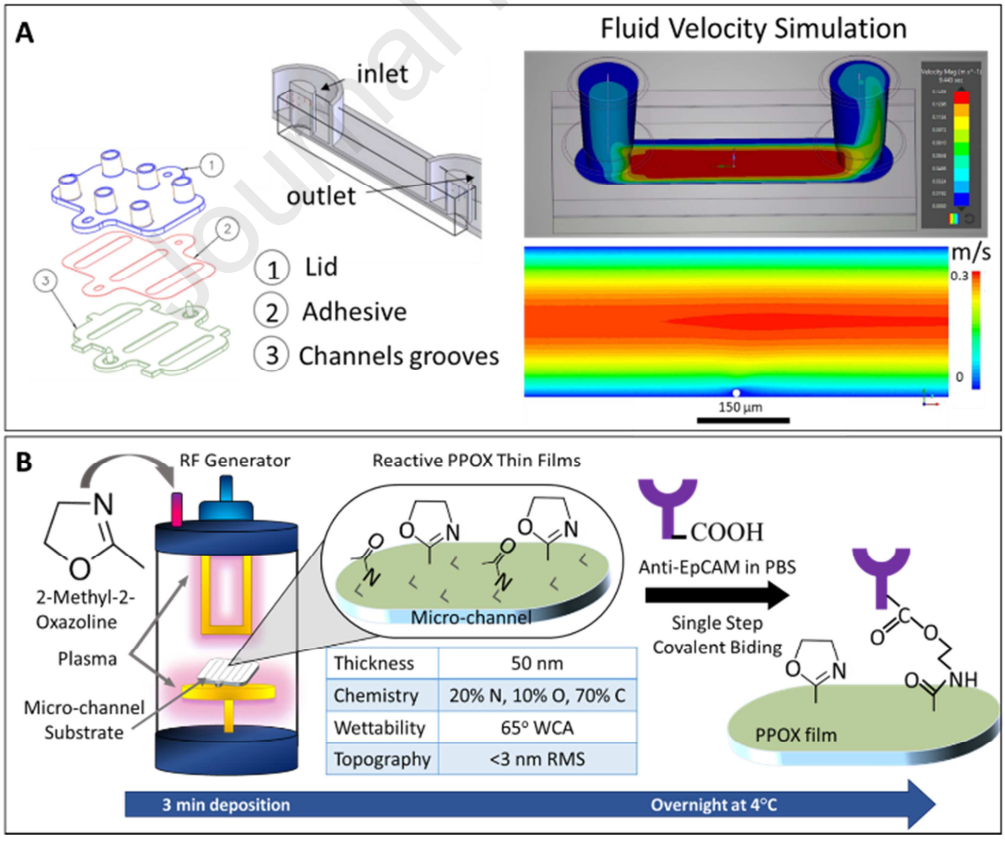

Figure 2. *A. Microfluidic device design, dimensions and fluid velocity contour (3D device scale profile and velocity magnitude in Y-Z plane) for an injection/rinsing rate of 10mL/min. B. Schematic of the diagnostic device functionalisation process with plasma deposited polyoxazoline coating and surface bound anti-EpCAM antibodies. Model system using cell lines to quantify the detection efficiency.*

Selective Capture Optimisation. The capture efficiency of the platform was initially optimised and quantified using four bladder cancer cell lines RT4, HT1197, HT1376 and EJ138. Human foreskin fibroblasts (HFF) were used as a negative control, referred to as "healthy" henceforth. In a first step, the different building blocks of the MicroUPSD immunosensor (EpCAM-assisted immunocapture, HAL-induced detection) have been assessed independently.

The selected cell lines were characterised for EpCAM expression via western blot, immunocytochemistry and flow cytometry (**Fig. 3A-C**). HT1197, HT1376 and RT4 expressed EpCAM while HFF and EJ138 did not. Other bladder cancer biomarkers including E-Cadherin (Bryan, 2015; Patriarca et al., 2009), and uroplakin (Hoang et al., 2014; Kaufmann et al., 2000) were also tested but were not chosen because their expression was inconsistent across all cancer cell lines investigated (**SupFig. 2**). From a range of commercially available options, we tested six different anti-EpCAM antibodies (**SupFig. 3**) and selected the best performing one, namely the polyclonal Goat anti-human EpCAM AF960, by R&D systems. It was paired with the best performing blocking agent, namely skim milk (Merck). (**SupFig. 3**). Captures rates obtained with EpCAM AF960 antibody as the selective capture ligand and skim milk solution as the non-specific binding blocking agent are shown in **Fig. 3D** for HT1376, HT1197 and RT4 cancer cell lines and HFF control cells. Absolute cell numbers are provided in **SupTable 1**. It is worth noting that in these experiments, as well as in previous spiked urine experiments (Macgregor-Ramiasa et al., 2017), every single cell captured in the channel was individually counted. In other words, the device is capable of detecting the presence of a single cell in the microchannel, that is one cell in 45 µL or

22 cells per mL. **SupVid 2** shows the real-time capture of cancer cells flowing over the EpCAM surface. The capture rates are defined as the percentage of all cell dispensed in the channels that remained bound after rinsing, which in the EpCAM-functionalised channel corresponds to the device sensitivity. On the block channel, used as negative control, less than 7% of all cell types remained bound after rinsing. In contrast, 100% of the cells remained non-specifically bound to the POx coating, as expected for this positive control surface. Less than 5% of the HFF cells remained bound to the anti-EpCAM functionalised channels, while for cancer cell lines the capture rate was 90% for HT1379, 96% for HT1197 and 99% for RT4, in good agreement with the EpCAM expression levels determined via FACS analysis.

PpIX fluorescence optimisation. The second selection criterion was for captured cells to display HAL-induced PpIX fluorescence. Cell line adherent monolayers were incubated with exogenous HAL to identify the optimal *ex vivo* processing conditions for HAL concentration and incubation time (**Fig. 3E-G**). The cancer cell lines displayed a higher mean PpIX fluorescence than the control HFF cells at all HAL concentrations investigated. A statistically significant difference in PpIX fluorescence intensity between healthy HFF and cancer cell lines was obtained after 2h incubation with 25 µM and 50 µM HAL.

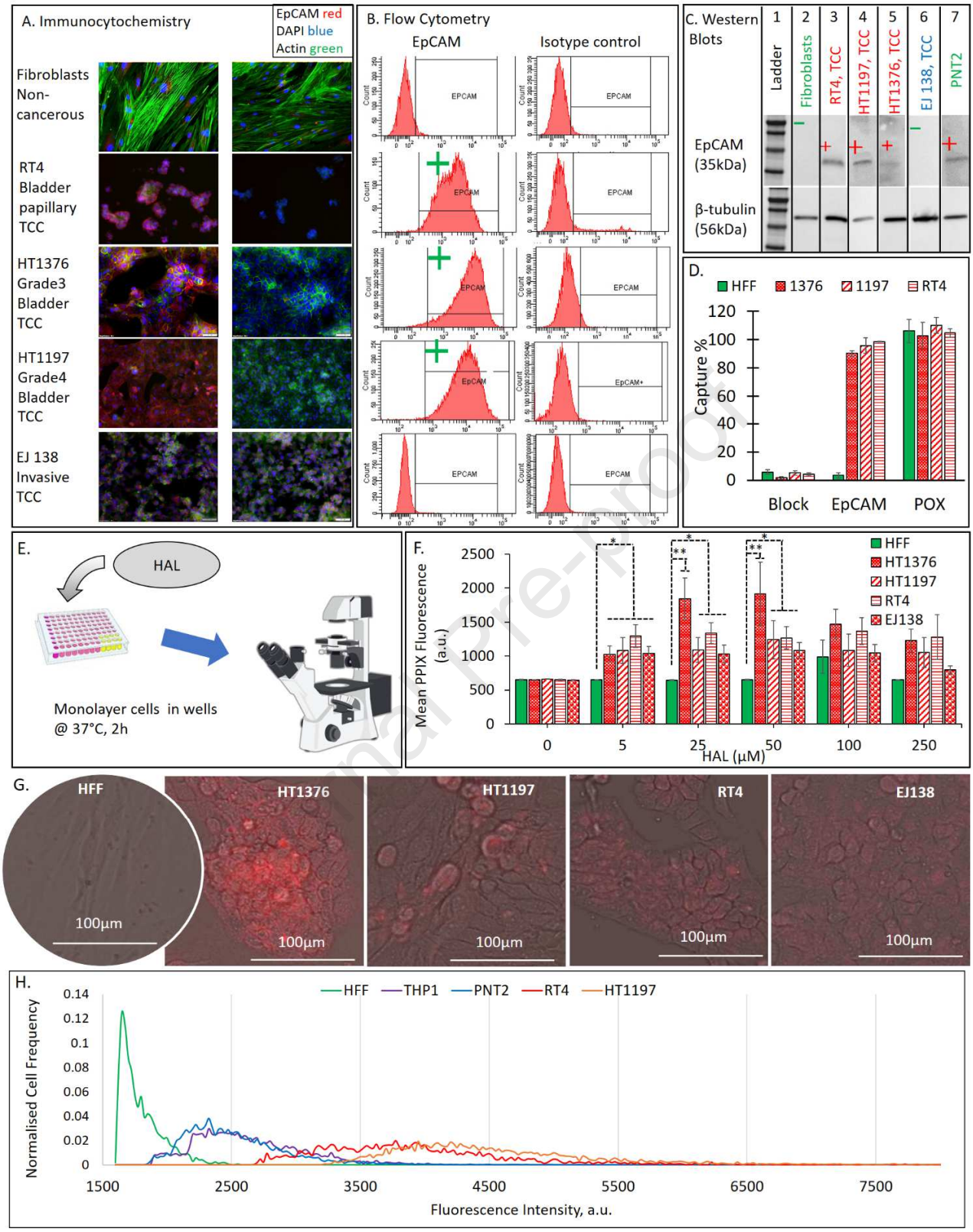

Figure 3. *Fibroblasts, RT4, HT-1197, HT-1376 and EJ138 EpCAM expression via A. Immunocytochemistry staining for DAPI, Phalloidin, and EpCAM. B. Flow Cytometry C. Western Blot for 30 μg protein loading. Top: EpCAM expression, and bottom protein loading control with β-tubulin. Lane 1: ladder. Column 7 is PNT2, prostate normal epithelial cells. D. Shows the capture rate of HFF (<5%) and HT1197, HT1376 and RT4 (>90%) in the optimised microUPSD device E. Schematic of cell preparation with HAL for Imaging. F. Mean HAL fluorescence of cell monolayers in human fibroblast (HFF) and four bladder cancer cell lines (HT1376, HT1197, RT4, EJ138), treated with 0-250μM of HAL for 2 hours. *=p<0.05, **=p<0.01. G. Red fluorescent PpIX observed in all bladder cancer cell lines but not in human fibroblast HFF cells under fluorescence microscopy, magnification 10x. H. Histogram of the HAL-induced PpIX fluorescence intensity of HFF, THP1 monocytes, PNT2 healthy epithelial cells compared to bladder cancer cell lines HT1197 and RT4 after 2h incubation.*

However, the overall PpIX fluorescence intensity varied between cell lines, HT1376 reaching **=*p<0.*01 while the other cancer cell lines reached *=*p<0.05* significance compared to HFF. A lowered HAL concentration (5 μM) did not lead to statistical differences between healthy and malignant cells while higher HAL concentrations (≥100 μM) were cytotoxic as seen in preliminary works (Casas et al., 2001; Chan et al., 2019). In order to closely mimic the use of HAL on cancer cells shed in urine samples, (Chan et al., 2020) HAL incubation conditions were tested on cells in suspension (**SupFig. 4**). Overall the fluorescence of cells in suspension was at least three-fold higher than for cell monolayers. In these conditions, the HAL concentration gradient had little effect on PpIX fluorescence intensity and cell integrity over the range investigated (10 – 150 μM). In fact, after as little as 30 minutes and up to 4 hours incubation with 50 μM HAL, the fluorescence intensity measured in cancer cells in suspension was significantly higher compared to that in fibroblasts ($p<0.0001$). These results indicate that when cells are in suspension, the PpIX fluorescence of bladder cancer cell lines is significantly stronger than

that of HFF over a wide range of HAL concentrations and incubation times. Similar results were obtained when comparing the HAL-induced fluorescence intensity of bladder cancer cell lines with primary normal bladder cells, both immobilised in POx-coated microchannels. (SupFig 5 A and B) It is worth noting, however, that HAL-induced PpIX fluorescence varies between cell types (Mateasik et al., 2017). We therefore tested additional non-malignant cell lines, representative of other cell types that are also expected to be found in urine samples; namely a healthy epithelial and a monocyte cell line, PNT2 and THP1, respectively. Histograms of PpIX fluorescence after 2h incubation with 50µM HAL are shown in **Fig. 3H**. Although there is a shift toward higher PpIX fluorescence intensity for PNT2 and THP1 compared to HFF, their mean fluorescence remains significantly lower than that of the cancer cell lines ($P<0.001$). (**SupFig. 5 C**).

The results for the cell line experiments demonstrated that the approach tested could efficiently and selectively isolate cancer cells based on their EpCAM expression and that HAL-induced fluorescence can be used to identify the captured cancer cells. These results, taken together, prompted us to proceed to evaluate the efficacy of the new sensor platform with clinical patient samples.

Clinical Study Having optimised the MicroUPSD platform with cell lines, we evaluated its capability for the detection of urological cancers in urine samples from patients with and without tissue-diagnosed bladder cancer. A total of 51 patients were enrolled from the urological service of Southern Adelaide Local Health Network (SALHN). All participants received study information and signed a consent form. The protocol for patient sample collection and testing was approved by the SALHN ethics committee. The mean age of the patients was 65, ranging from 34 to 94 years old. 27% of participants were female. The assay was tested using patients with a range urogenital disorders including benign urinary tract infection, calculi, prostatic hyperplasia. This patient cohort had a clinical indication for cystoscopic examination with a broad range of clinical pathologies including bladder cancer. All clinical information re-

garding the patient cohort are provided in **SupTables 2 and 3** for the optimisation and validation cohorts, respectively.

The optimisation cohort, consisting of 16 patients, was used to define the incubation time and threshold for HAL-induced fluorescence detection. 50 mL of voided urine sample was collected just before cystoscopy, stored at 4 ^{o}C and processed within 5 hours after collection. 5 mL of urine was centrifuged at 20,000 X g, the supernatant discarded and the remaining 300 µL of cell-containing urine was incubated for either 1h or 2h at room temperature with HAL (50 µM). The cell suspension was then introduced in the MicroUPSD channels and left to interact with the substrates for 45 min before applying a 1 mL PBS rinse. Some of the cells captured in the EpCAM-functionalised channel featured morphological characteristic consistent with malignant cells (transitional cell clusters, high nuclear/cytoplasmic ratio, nuclear membrane irregularities(Zink et al., 2004)) (**Fig. 4A**). However, the absolute number of cells captured, ranging from 10 to 260 per channel, did not directly correlate with the histopathology results (**SupFig. 6A**). While the EpCAM-based capture is intended to enrich the population of cancer cells by depleting EpCAM-negative cells found in urine, healthy epithelial cells may also bind to the surface. These results corroborated the need for HAL-induced PpIX fluorescence as an additional detection criterion. Histograms of the mean fluorescence intensity of each cell captured in the EpCAM channel were generated, **Fig. 4B** and **SupFig. 6BC**, and the median fluorescence intensity of the captured cell population for each patient was calculated from experimental duplicate (**Fig. 4C**).An overall shift towards higher fluorescence intensity is seen in the histogram of patients with cancer, which translated to a small statistical difference in the median fluorescence of cancer compared to control patients for both 1h and 2h incubation time with HAL, $p=0.052$ and $p=0.008$, respectively. In order to further correct for the presence of healthy epithelial cells which have lower PpIX fluorescence intensity than malignant cells, the number of cells displaying fluorescence levels above increasing thresholds of intensity were interrogated. Fluorescence intensity thresholds with cut-off values of 3000, 3500, 4000, 4500 and 5000 were

systematically tested, **SupFig. 6DE**. Comparing these results with the histopathological diagnosis, a threshold of 4000 a.u. was identified as the most suitable to discriminate cancer cases from benign conditions after 1h incubation with HAL (p=0.07). This result is in good agreement with the observations from the cell line capture experiments, where none of the non-malignant cell types displayed fluorescence above 4000 a.u. The presence of cells with low PpIX fluorescence intensity in the urine of patients may be attributed to a residual non-specific binding of non-malignant cells; typically less than 5% according to the *in vitro* test results. To correct for this effect, the number of cells bound to the blocked microchannel (negative control) was used as a baseline in the validation cohort.

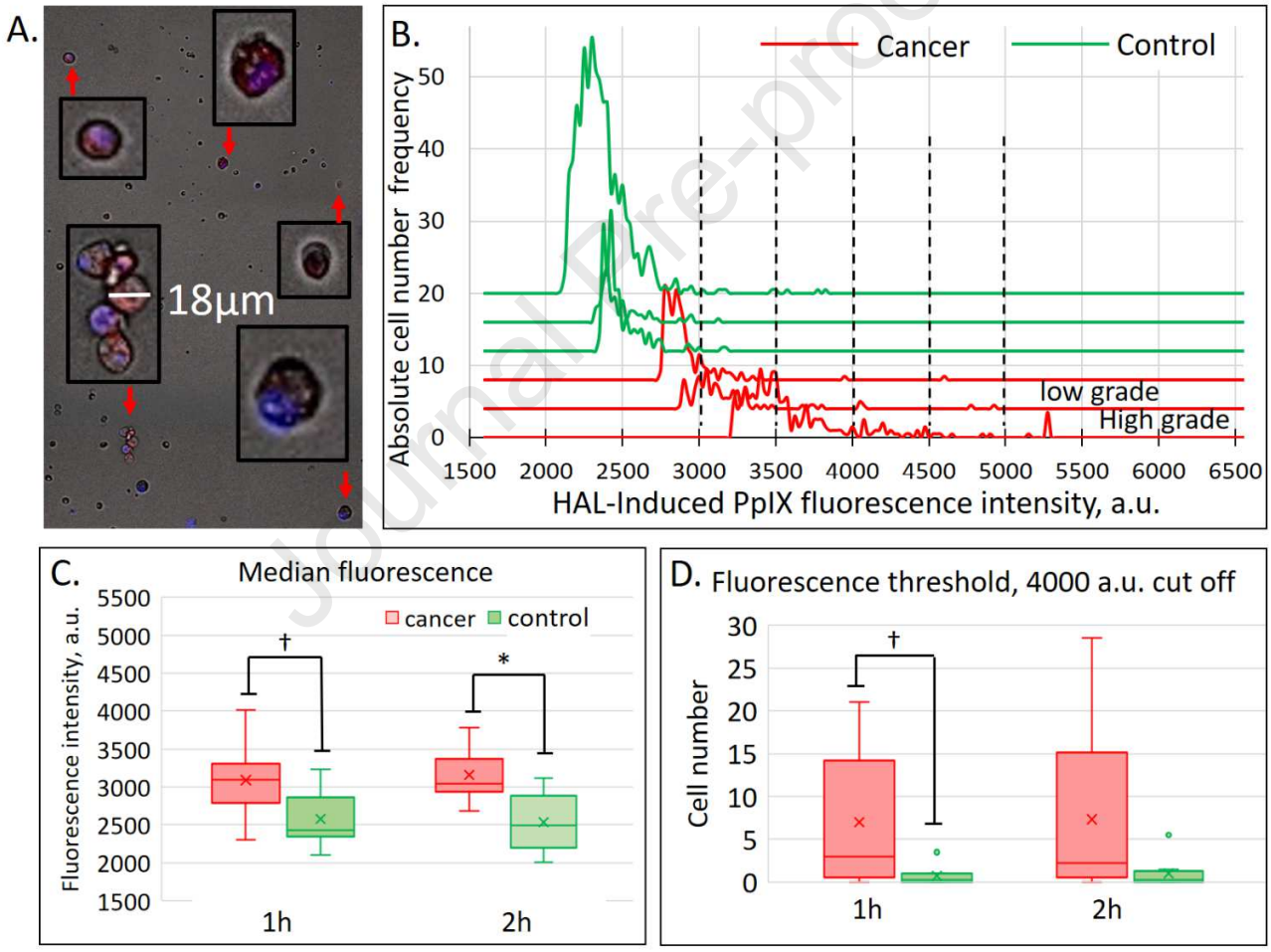

***Figure 4**. HAL-induced fluorescence in patient samples. A. micrograph of captured cells featuring morphological characteristics consistent with malignant cells (cell clusters, large nuclei compare to cyto-*

*plasm visible with nuclear stain in blue). B. Histogram of the mean HAL-induced PpIX fluorescence intensity of the captured cells. (x axis, absolute number of cells) C. Box plot of the median fluorescence of the captured cell population calculated from the histogram data. D. Number of cells with mean fluorescence above 4000 a.u. intensity threshold. (†=p<0.1, * =p<0.1)*

Having established a fluorescence intensity threshold in the optimisation cohort, we moved on to assess test performance in the validation cohort. The validation cohort consisted of 35 patients undergoing cystoscopy for a variety of clinical indications. 6 patients had histopathologically confirmed bladder cancer, 3 had prostate cancer and 1 with bowel cancer which had invaded the bladder wall. The results from the MicroUPSD test were compared with those of the histopathology, cystoscopy and cytology examination, as illustrated in **Fig. 5A**. Resected tumours or biopsy were histologically examined, staged and graded according to the Royal College of Pathologists of Australasia classification system.(Grignon D, 2018) **SupTable 3** show results of cytology, cystoscopy and histopathology, used here as the gold standard for pathological confirmation of urothelial carcinoma.

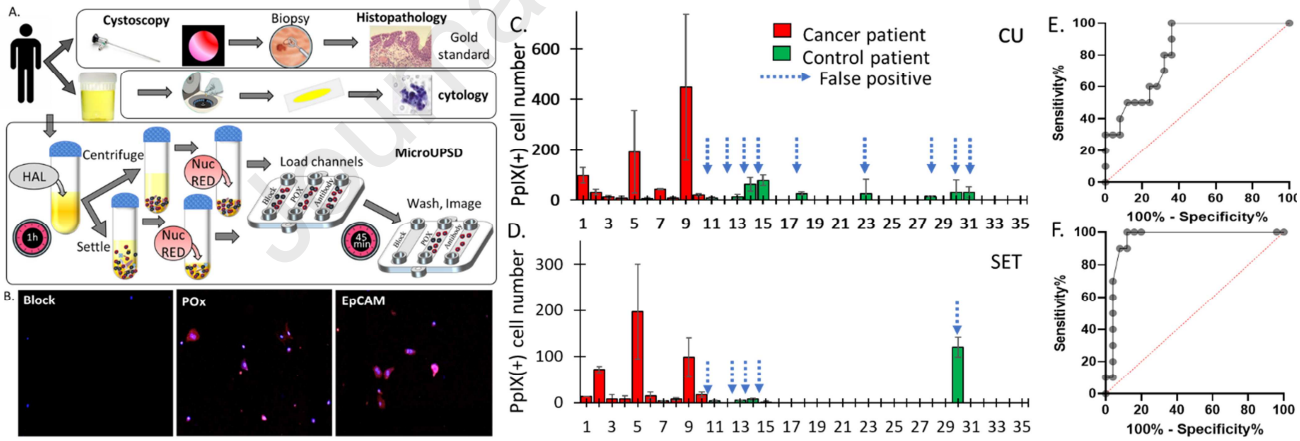

Figure 5. *A. Flow diagram depicting the steps undertaken in conventional diagnostic methods including cytology, cystoscopy and histopathology as well as in the MicroUPSD approach. B. Representative fluorescent micrograph of cells found in the Block, Pox and EpCAM microchannels, C. and D. Results of the MicroUPSD test, showing the difference in absolute numbers of PpIX positive cells between the EpCAM*

and block channel, for centrifuged (CU) and settled (SET) urine samples respectively. E. and F. ROC curve for illustration of the MicroUPSD performance in the discrimination of cancer from benign conditions for centrifuged (AUROC=0.824, 95% CI 0.6863 to 0.9617, P=0.003) and settled (AUROC=0.952, 95% CI 0.8780 to 1.000, P<0.0001) patient samples.

The number of exfoliated cells in urine is a known limiting factor for urinary based diagnostic methods. Thus, to increase cell concentration, urine samples are routinely centrifuged for cytological examination. However, centrifugation has the disadvantage of damaging cell integrity and concentrating non-specifically all material present in the urine with a higher density than the liquid. A gentler alternative could be settling the patient samples (Grover et al., 2011; Shaw Bagnall et al., 2015). To test this hypothesis, two sample preparation methods were used as detailed in Fig. 5A. Objects captured in the anti-EpCAM functionalised channel with diameters between 7 and 53 µm and displaying co-localised NuclearRed and HAL-induced PpIX fluorescence were counted as cancer cells. **Fig. 5B** shows representative images of the cell population found in the block, POx and EpCAM microchannel. The difference in the absolute numbers of cells captured in the EpCAM and blocked channel are reported in **Fig. 5C** and **Fig. 5D** for the Centrifuged (CU) and settled (SET) urine samples, respectively. We evaluated the reproducibility of the detection methods using split samples and showed satisfactory reproducibility. Error bars in Fig. 5C and D were derived from these two technical replicates. Sensitivity, specificity, positive predictive value (PPV), and negative predictive value (NPV) were calculated using equations 1-4, defined in supplementary infomation. The clinical gold standard diagnostic is WLC followed by biopsy and histopathological examination if a lesion is present. The contingency table (Table 1) summarises the detection performance of the MicroUPSD test chip, cytology and cystoscopy compared to the gold standard. It is worth noting that cystoscopy alone is not used to define diagnosis in clinical settings. Nonetheless, for the statistical analysis, we here evaluated the capacity of cystoscopic examination at identifying suspicious lesions. In **Table 1**, a WLC result was considered positive if the findings warrant-

ed a biopsy and histopathology examination. In this instance, a MicroUPSD test is recorded as positive if there are more PpIX positive cells captured in the EpCAM channel than in the negative control block channel.

No cancer cases were missed using the MicroUPSD (i.e. sensitivity and NPV was 100%), for both the SET and CU urine processing approaches. In comparison, the sensitivity of cytology was only 20%, with 8 false negatives and an NPV of 76%. On the other hand, specificity and PPV were different for SET and CU. Centrifugation of the urine samples led to 64% specificity and 53% PPV, while settled urine sample achieved higher specificity and PPV of 80% and 67%. The test accuracy in settled urine samples implies that the proposed MicroUPSD approach could be used with un-processed urine samples, outside of pathology labs. This could be particularly beneficial for its integration in point of care devices, typically used where centrifugation is not available in a non-hospital setting. Overall, the microfluidic test detected 8 cancers that conventional cytology failed to identify and had false-positive rates similar to those of cystoscopy.

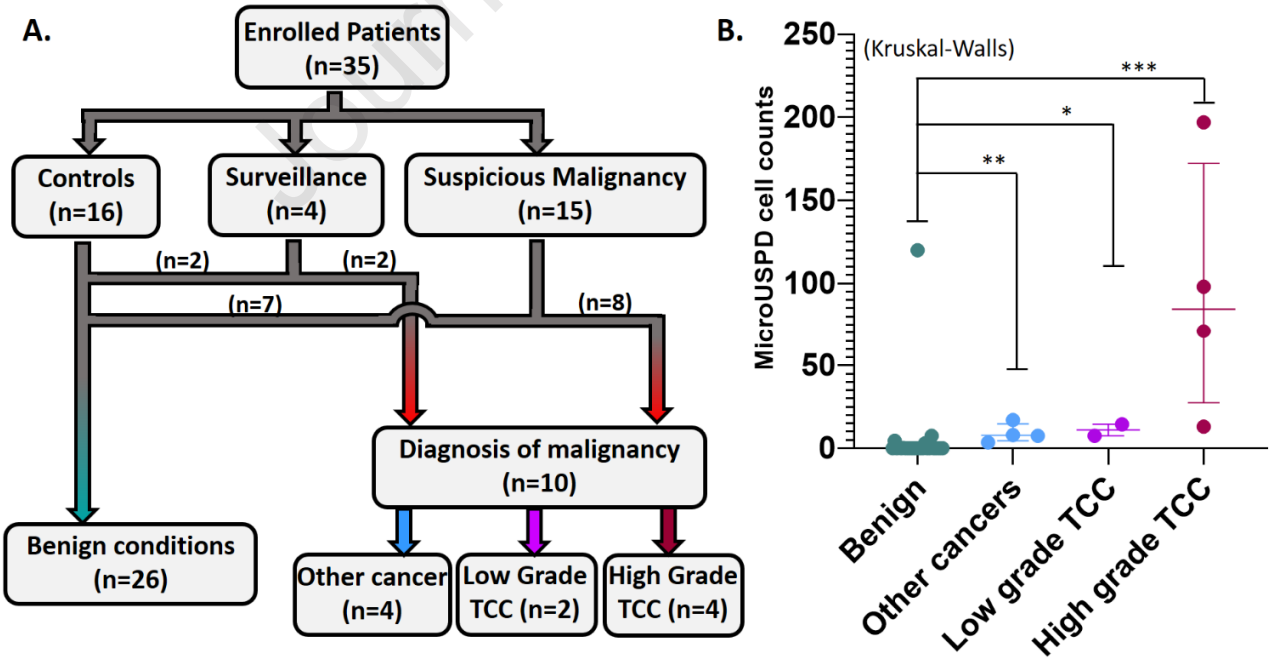

Figure 6: A. Flowchart of the pilot study showing the partition of control and cancer cases participating in the validation cohort. B. Results of the MicroUPSD for the validation cohort, showing cell counts for control patient with benign conditions, patients with malignancy other than TCC of the bladder, as well as patient with low and high grade TCC. Detailed results of the statistical analysis performed with a Kruskal-Walls test) are provided in **SupTable 4**.

Further statistical analysis was performed by interrogating the absolute number of PpIX positive cells that were selectively captured in the EpCAM channel with co-localised NuclearRed staining. ROC curves were constructed taking increasing numbers of selectively captured PpIX cells as cut off values**, Fig. 5E and F.** Values of 88% specificity and 100% sensitivity were achieved for the SET urine samples with a cut off value of three cells or more. This is because false positive cases generally had low numbers of cells captured. Considering the actual number of captured cells displaying co-localised PpIX and NuclearRed fluorescence, statistically significant differences were noted between low- and high-grade cancer versus non-cancerous controls (Fig. 6). The average number of selectively captured cells was 98 for confirmed high grade cancers cases (n=4) and 5 for non-cancerous patients.

Table 1: *Contingency table comparing the performance pf cystoscopy, cytology, and Micro UPPD for both SET and CU processed urine, with the histopathology gold standard. *4 patient did not undergo cystoscopic examination.*

	Gold Standard Histopathology				
		+	-		
MicroUPSD CU	+	10	9	19	**PPV= 0.526**
	-	0	16	16	**NPV= 1.000**
		10	25	35	**Sensitivity 1.000**
					Specificity 0.640
		+	-		**PPV= 0.667**
MicroUPSD SET	+	10	5	15	**NPV= 1.000**
	-	0	20	20	**Sensitivity 1.000**
		10	25	35	**Specificity 0.800**
		+	-		**PPV= 1.000**
Cytology	+	2	0	2	**NPV= 0.758**
	-	8	25	33	**Sensitivity 0.200**
		10	25	35	**Specificity 1.000**
		+	-		**PPV= 0.438**
Cystoscopy*	+	7	9	16	**NPV= 1.000**
	-	0	15	15	**Sensitivity 1.000**
		7	24	31	**Specificity 0.625**

4. Discussion

The diagnostic device that was developed using cultured cells performed well with actual patient urine samples. In a small pilot cohort, it achieved excellent sensitivity for cancer detection with, however, imperfect specificity. The false-positive results obtained with the MicroUPSD did not correlate with gender, or time taken from collection to analysis. Importantly, all false positive cases had moderate to high leucocyte counts in the dipstick urine analysis test, however, not all cases of high leucocyte counts led to false positives, with 6 of the true negatives also having high leucocyte counts. Autofluorescence of cells is a well-known phenomenon which appears to be more pronounced in immune cells (Monici et al., 1995; Wizenty et al., 2018). Here, it may be responsible for the false positive cases recorded in patients with high leucocyte counts. Another factor may be the uptake of HAL by immune cells. In cell

line experiments, we observed that monocytes displayed higher HAL-induced PpIX fluorescence than other non-malignant cell types such as fibroblasts (Fig. 3H). When the initial cellularity of the samples was particularly high, the non-specific binding of immune cells could be a limiting factor for the MicroUPSD detection approach. This could explain why the number of false positives decreased by almost half in the settling approach, which involves a 1:1 dilution in PBS; resulting in a lower number of cells entering the microchannel. The variability in the absolute number of cells shed in the urine represent a challenge for the MicroUPSD approach, as well as related aspects including the need to process the sample while fresh to avoid cell deterioration. These limitations may potentially be overcome by introducing different urine processing steps (such as tailored dilution or concentration to a set cell concentration) prior to introduction in the device.

Furthermore, strategies involving hardware automation and software refinement could be implemented to further reduce the false positive rates. The size selection criteria used in this work (7-53 µm in diameter), for instance, were more permissive than those used in commercial CTC-capture devices such as ISET Rarecell (Farace et al., 2011; Shashni et al., 2018; Vona et al., 2000). The cut-off size of 53 µm was chosen to include as many diagnostically informative cells while excluding aggregates, large umbrella cells and casts debris. Nonetheless, the presence in urine of normal epithelial cells represent a challenge for size-based selection, as many of these cells overlap in size with carcinoma cells which calls for additional selection criteria. (Andersson et al., 2014) For instance, although the size distribution of leucocytes overlaps with that of cancer cells, it has been shown that they are more deformable due to their smaller nucleus size (Phillips et al., 2012). Therefore, adding a specific selection criterion for nucleus size and cell shape could further narrow the distinction between cancer and immune cells in future works.

The bladder cancer cell detection approach developed in this work is based on the overexpression of EpCAM. While this is arguably the most studied and diagnostically useful cancer-specific antigen, it is not specific for bladder cancer. As a result, any EpCAM expressing cancer cell present in urine could be detected. Indeed, in this study cohort, three prostate cancers were detected in the MicroUPSD as well as a colon cancer case where the tumour had invaded the bladder wall. Though, the actual number of cells captured for these four "other cancer" cases was lower than in high grade bladder cancer cases. Further investigations in a larger patient cohort will be required to determine if this approach can reliably detect other cancers of different epithelial origin that shed EpCAM-positive cells in the urine and to more precisely determine test sensitivity. A positive result from the MicroUPSD test would therefore require the clinician to consider the origin of the malignancy in the subsequent management of the patient treatment plan. Using EpCAM as the capture antibody also means that malignant cells which have undergone epithelial to mesenchymal transition may be missed.(Hyun et al., 2016) As observed in the cell line experiments, bladder cancer line EJ136 did not express EpCAM. Unlike HT1197 (grade 4 TCC), HT1376 (grade 3 carcinoma) and RT4 (transitional cell papilloma) EJ138 originate from an invasive TCC. These cells may have undergone the epithelial to mesenchymal transition often associated with metastasis which would explain a loss in EpCAM expression. Indeed, loss of cell adhesion have been reported in high grade bladder tumour cells. Caused by E-cad and beta-cathenin gene loss, lower cell adhesion was identify as one possible reason for higher shedding in urine(Hu et al., 2011; Miyake et al., 2014) While no false negative cases were recorded in the cohort investigated here, future development of the microUSPD could involve adding a complementary anti-body to either or both specifically target bladder or high metastatic cancer cells.

Future work will focus on exploring the potential of the microUSPD approach for detecting the extreme end of the spectrum, namely aggressive, advanced cancer that may not express EpCAM but also low grade cancers which potentially shed much less cells in the urine. While the preliminary results ob-

tained here and summarized in figure 6 are promising, a full scale clinical study would be required to assess the potential implication the microUSPD could have on disease management.

5. Conclusions

Current bladder cancer diagnostic methods are invasive. Existing non-invasive approach such as cytology or urinary biomarker detection, have limitations in terms of specimen preparation complexity, analysis costs and overall low sensitivity that preclude them from replacing cystoscopies. The technology developed in this work allows for the non-invasive detection of bladder cancer from non-processed urine samples. An immunoaffinity-based microfluidic platform was successfully used to concentrate exfoliated cancer cells without the need to centrifuge the urine specimen first, thereby overcoming existing limitation of urine cytology. Next, HAL was used to induce cancer specific PpIX fluorescence, and a swift analysis protocol was established which enabled the identification of individual cancer cells based on their fluorescence intensity profile. This new procedure allows for the detection of cancer cells without expensive PCR equipment and reagents, thus overcoming limitation faced by omics-based urinary tests. In this preliminary study, the test detected all cancer cases, with a NPV of 1 and a specificity of 80%. The diagnostic accuracy is sufficiently high for this approach to be considered for a larger clinical trial to examine its potential at detecting urogenital cancers which shed cancer cells into urine. The method can pave the foundation of future non-invasive and cost-effective surveillance tools for urinary cancers to be adopted in clinical practice.

SUPPORTING INFORMATION.

Flow analysis in microchannel, detailed methods for flow cytometry, immunohistochemistry, western blot and statistical calculation with additional data. Coatings physicochemical characteristaion. Results from commercial antibody and blocks tests. Cell capture cell numbers and real time video. HAL-

induced fluorescence analysis for cell lines in suspension. Clinical data for optimization and validation patients cohorts.

ACKNOWLEDGMENT

The authors acknowledge the financial support from UniSA Research theme Investment grant, and the commonwealth CRC-Project scheme. The CRC Programme supports industry-led collaborations between industry, researchers and the community.

The authors acknowledge the instruments and scientific and technical assistance of Microscopy Australia at the Future Industries Institute, University of South Australia, a facility that is funded by the University, and State and Federal Governments. This work was performed (in part) at the South Australian node of the Australian National Fabrication Facility under the National Collaborative Research Infrastructure Strategy.

AUTHOR CONTRIBUTIONS.

MM contributed to the conception and design of the study, established experimental protocols, analysed and interpreted the data and wrote the manuscript with input from all authors. **HSS** processed clinical samples, contributed to data analysis, and assisted with the initial paper drafting. **KMC** provided the cells for cell lines experiments, conducted HAL optimisation experiments, assisted in the testing of patient samples, data analysis and drafting of the paper. **KO** assisted with cell culture, conducted cell line experiments and assisted with patient samples processing**. KM** assisted with cell culture, contributed to study design, conducted western blotting experiments and reviewing the paper**. AHS** performed sample analysis by flow cytometry and data analysis and editing of the paper**. TDM** contributed to sample testing of cell lines, data analysis and editing of the paper. **AZ** contributed to sample preparation and assisted the testing of clinical samples. **MPB** contributed to study design and editing of the paper. **MNK** conducted the simulation of fluid flow, contributed to the fluid dynamics analysis in the microfluidic device

and writing the paper. **AJ** and **MC** conducted the clinical diagnosis of the patients and contributed to the editing of the paper. **ADF** and **AG** contributed to the microfluidic chip design, established its fabrication facilities, and contributed to experiment planning**. SR** developed macros for image processing software**. SB** contributed to experiment design, supervision and project administration. **JL** contributed to study design, ethics application, patient recruitment, data interpretation and reviewing the paper. **JG** contributed to the conception, design, patient recruitment, data interpretation and drafting of the paper. **KV** contributed to the conception, design and validation of the work, supervision and project administration as well as writing, reviewing and editing the paper.

‡These authors contributed equally.

REFERENCES

Andersson, E., Steven, K., Guldberg, P., 2014. Size-Based Enrichment of Exfoliated Tumor Cells in Urine Increases the Sensitivity for DNA-Based Detection of Bladder Cancer. PLoS One 9(4), e94023.
Arya, S.K., Lim, B., Rahman, A.R.A., 2013. Enrichment, detection and clinical significance of circulating tumor cells. Lab on a Chip 13(11), 1995-2027.
Babjuk, M., Böhle, A., Burger, M., Capoun, O., Cohen, D., Compérat, E.M., Hernández, V., Kaasinen, E., Palou, J., Rouprêt, M., van Rhijn, B.W.G., Shariat, S.F., Soukup, V., Sylvester, R.J., Zigeuner, R., 2017. EAU Guidelines on Non Muscle-invasive Urothelial Carcinoma of the Bladder: Update 2016. Eur. Urol. 71(3), 447-461.
Barkan, G.A., Wojcik, E.M., Nayar, R., Savic-Prince, S., Quek, M.L., Kurtycz, D.F.I., Rosenthal, D.L., 2016. The Paris System for Reporting Urinary Cytology: The Quest to Develop a Standardized Terminology. Acta Cytol. 60(3), 185-197.
Bell, M.D., Yafi, F.A., Brimo, F., Steinberg, J., Aprikian, A.G., Tanguay, S., Kassouf, W., 2016. Prognostic value of urinary cytology and other biomarkers for recurrence and progression in bladder cancer: a prospective study. World J. Urol. 34(10), 1405-1409.
Biardeau, X., Lam, O., Van Ba, L.C., Corcos, J., 2017. Prospective evaluation of anxiety, pain, and embarrassment associated with cystoscopy and urodynamic testing in clinical practice. Canadian Urological Association Journal 11(3-4), 104.
Bryan, R.T., 2015. Cell adhesion and urothelial bladder cancer: the role of cadherin switching and related phenomena. Philosophical Transactions of the Royal Society B: Biological Sciences 370(1661).
Bryan, R.T., Shimwell, N.J., Wei, W., Devall, A.J., Pirrie, S.J., James, N.D., Zeegers, M.P., Cheng, K.K., Martin, A., Ward, D.G., 2014. Urinary EpCAM in urothelial bladder cancer patients: characterisation and evaluation of biomarker potential. Br. J. Cancer 110(3), 679-685.
Bubendorf, L., Caraway, N.P., Fischer, A.H., Katz, R.L., Olson, M.T., Schmitt, F., Fležar, M.S., Van Der Kwast, T.H., Vielh, P., 2016. Ancillary studies in urinary cytology, The Paris System for Reporting Urinary Cytology. Springer, pp. 115-136.

Casas, A., Fukuda, H., Di Venosa, G., Batlle, A., 2001. Photosensitization and mechanism of cytotoxicity induced by the use of ALA derivatives in photodynamic therapy. Br. J. Cancer 85(2), 279-284.

Cavallaro, A.A., Macgregor-Ramiasa, M.N., Vasilev, K., 2016. Antibiofouling properties of plasma-deposited oxazoline-based thin films. ACS applied materials & interfaces 8(10), 6354-6362.

Chakraborty, A., Dasari, S., Long, W., Mohan, C., 2019. Urine protein biomarkers for the detection, surveillance, and treatment response prediction of bladder cancer. Am. J. Cancer Res. 9(6), 1104-1117.

Chakraborty, A., Dasari, S., Long, W., Mohan, C., 2019. Urine protein biomarkers for the detection, surveillance, and treatment response prediction of bladder cancer. American journal of cancer research 9(6), 1104-1117.

Chan, K.M., Gleadle, J., Vasilev, K., MacGregor, M., 2020. Probing Hexaminolevulinate Mediated PpIX Fluorescence in Cancer Cell Suspensions in the Presence of Chemical Adjuvants. International Journal of Molecular Sciences 21(8), 2963.

Chan, K.M., Vasilev, K., Shirazi, H.S., McNicholas, K.Y.M., Li, J., Gleadle, J., Macgregor, M., 2019. Biosensor device for the photo-specific detection of immuno-captured bladder cancer cells using hexaminolevulinate: An ex-vivo study. Photodiagnosis Photodyn. Ther. 28, 238-247.

Chan, K.M.G., J.; Li, J.; Vasilev, K.; MacGregor, M., 2020. Shedding Light on Bladder Cancer Diagnosis in Urine. Diagnostics 10(6), 383.

Dinges, S.S., Hohm, A., Vandergrift, L.A., Nowak, J., Habbel, P., Kaltashov, I.A., Cheng, L.L., 2019. Cancer metabolomic markers in urine: evidence, techniques and recommendations. Nature reviews. Urology 16(6), 339-362.

Dinney, C.P.N., McConkey, D.J., Millikan, R.E., Wu, X., Bar-Eli, M., Adam, L., Kamat, A.M., Siefker-Radtke, A.O., Tuziak, T., Sabichi, A.L., Grossman, H.B., Benedict, W.F., Czerniak, B., 2004. Focus on bladder cancer. Cancer Cell 6(2), 111-116.

Farace, F., Massard, C., Vimond, N., Drusch, F., Jacques, N., Billiot, F., Laplanche, A., Chauchereau, A., Lacroix, L., Planchard, D., Le Moulec, S., André, F., Fizazi, K., Soria, J.C., Vielh, P., 2011. A direct comparison of CellSearch and ISET for circulating tumour-cell detection in patients with metastatic carcinomas. Br. J. Cancer 105(6), 847-853.

Frantzi, M., van Kessel, K.E., Zwarthoff, E.C., Marquez, M., Rava, M., Malats, N., Merseburger, A.S., Katafigiotis, I., Stravodimos, K., Mullen, W., Zoidakis, J., Makridakis, M., Pejchinovski, M., Critselis, E., Lichtinghagen, R., Brand, K., Dakna, M., Roubelakis, M.G., Theodorescu, D., Vlahou, A., Mischak, H., Anagnou, N.P., 2016. Development and Validation of Urine-based Peptide Biomarker Panels for Detecting Bladder Cancer in a Multi-center Study. Clinical cancer research : an official journal of the American Association for Cancer Research 22(16), 4077-4086.

Gallagher, K.M., Gray, K., Anderson, C.H., Lee, H., Stewart, S., Donat, R., Mariappan, P., 2017. 'Real-life experience': recurrence rate at 3 years with Hexvix((R)) photodynamic diagnosis-assisted TURBT compared with good quality white light TURBT in new NMIBC-a prospective controlled study. World J. Urol. 35(12), 1871-1877.

Geavlete, B., Geavlete, P.A., Georgescu, D., Mulțescu, R., Jecu, M., 2016. Chapter 2 - Fluorescence Cystoscopy, in: Geavlete, P.A. (Ed.) Endoscopic Diagnosis and Treatment in Urinary Bladder Pathology. Academic Press, San Diego, pp. 25-63.

Grignon D, B.F., Comperat E, Delahunt B, Koch M, Lopez-Beltran A, Reuter V, Samaratunga H, Shanks J, Tsuzuki T, van der Kwast T, Varma M, Srigley JR., 2018. Urinary Tract Carcinoma, Histopathology Reporting Guide, Biopsy and Transurethral Resection Specimen, 1st edition ed, Sydney, Australia.

Grover, W.H., Bryan, A.K., Diez-Silva, M., Suresh, S., Higgins, J.M., Manalis, S.R., 2011. Measuring single-cell density. Proc. Natl. Acad. Sci. U.S.A. 108(27), 10992-10996.

Hoang, L.L., Tacha, D.E., Qi, W., Yu, C., Bremer, R.E., Chu, J., Haas, T.S., Cheng, L., 2014. A newly developed uroplakin II antibody with increased sensitivity in urothelial carcinoma of the bladder. Arch. Pathol. Lab. Med. 138(7), 943-949.

Hu, X., Ruan, Y., Cheng, F., Yu, W., Zhang, X., Larré, S., 2011. p130Cas, E-cadherin and β-catenin in human transitional cell carcinoma of the bladder: Expression and clinicopathological significance. Int. J. Urol. 18(9), 630-637.

Hyun, K.-A., Koo, G.-B., Han, H., Sohn, J., Choi, W., Kim, S.-I., Jung, H.-I., Kim, Y.-S., 2016. Epithelial-to-mesenchymal transition leads to loss of EpCAM and different physical properties in circulating tumor cells from metastatic breast cancer. Oncotarget 7(17).

Jordan, B., Meeks, J.J., 2019. T1 bladder cancer: current considerations for diagnosis and management. Nature Reviews Urology 16(1), 23-34.

Jung, A., Nielsen, M.E., Crandell, J.L., Palmer, M.H., Bryant, A.L., Smith, S.K., Mayer, D.K., 2019. Quality of Life in Non-Muscle-Invasive Bladder Cancer Survivors: A Systematic Review. Cancer Nursing 42(3), E21-E33.

Kaufmann, O., Volmerig, J., Dietel, M., 2000. Uroplakin III Is a Highly Specific and Moderately Sensitive Immunohistochemical Marker for Primary and Metastatic Urothelial Carcinomas. Am. J. Clin. Pathol. 113(5), 683-687.

Khoo, B.L., Bouquerel, C., Durai, P., Anil, S., Goh, B., Wu, B., Raman, L., Mahendran, R., Thamboo, T., Chiong, E., Lim, C.T., 2019. Detection of Clinical Mesenchymal Cancer Cells from Bladder Wash Urine for Real-Time Detection and Prognosis. Cancers (Basel) 11(9), 1274.

Kiyoshima, K., Akitake, M., Shiota, M., Takeuchi, A., Takahashi, R., Inokuchi, J., Tatsugami, K., Yokomizo, A., Eto, M., 2016. Prognostic Significance of Preoperative Urine Cytology in Low-grade Non-muscle-invasive Bladder Cancer. Anticancer Res. 36(2), 799-802.

Lotan, Y., Bivalacqua, T.J., Downs, T., Huang, W., Jones, J., Kamat, A.M., Konety, B., Malmström, P.-U., McKiernan, J., O'Donnell, M., Patel, S., Pohar, K., Resnick, M., Sankin, A., Smith, A., Steinberg, G., Trabulsi, E., Woods, M., Daneshmand, S., 2019. Blue light flexible cystoscopy with hexaminolevulinate in non-muscle-invasive bladder cancer: review of the clinical evidence and consensus statement on optimal use in the USA — update 2018. Nature Reviews Urology 16(6), 377-386.

Lotan, Y., Roehrborn, C.G., 2003. Sensitivity and specificity of commonly available bladder tumour markers versus cytology: results of a comprehensive literature review and meta-analyses. Urology 61.

MacGregor-Ramiasa, M., Cavallaro, A., Visalakshan, R., Gonzalez, L., Vasilev, K., 2016. Plasma deposited polyoxazoline coatings, a versatile new class of biomaterials. Chemeca 2016: Chemical Engineering-Regeneration, Recovery and Reinvention, 302.

Macgregor-Ramiasa, M., McNicholas, K., Ostrikov, K., Li, J., Michael, M., Gleadle, J.M., Vasilev, K., 2017a. A platform for selective immuno-capture of cancer cells from urine. Biosens. Bioelectron.

Macgregor-Ramiasa, M., McNicholas, K., Ostrikov, K., Li, J., Michael, M., Gleadle, J.M., Vasilev, K., 2017b. A platform for selective immuno-capture of cancer cells from urine. Biosens. Bioelectron. 96, 373-380.

Macgregor-Ramiasa, M.N., Cavallaro, A.A., Vasilev, K., 2015. Properties and reactivity of polyoxazoline plasma polymer films. Journal of Materials Chemistry B 3(30), 6327-6337.

Macgregor, M.N., Michelmore, A., Safizadeh Shirazi, H., Whittle, J., Vasilev, K., 2017. Secrets of Plasma-Deposited Polyoxazoline Functionality Lie in the Plasma Phase. Chem. Mater. 29(19), 8047-8051.

Mateasik, A., Trnka, M., Kajo, K., Vallova, M., Cunderlikova, B., 2017. Cell-type dependent response to photodynamic treatment in 3D collagen cell cultures. Journal of photochemistry and photobiology. B, Biology 166, 94-103.

McGrew, E.A., 1961. The Role of Exfoliative Cytology in the Diagnosis and Treatment of Malignant Disease. Postgrad. Med. J. 37(430), 456-467.
McNicholas, K., MacGregor, M.N., Gleadle, J.M., 2019. In order for the light to shine so brightly, the darkness must be present—why do cancers fluoresce with 5-aminolaevulinic acid? Br. J. Cancer.
Miyake, M., Nakai, Y., Anai, S., Tatsumi, Y., Kuwada, M., Onishi, S., Chihara, Y., Tanaka, N., Hirao, Y., Fujimoto, K., 2014. Diagnostic approach for cancer cells in urine sediments by 5-aminolevulinic acid-based photodynamic detection in bladder cancer. Cancer Sci. 105(5), 616-622.
Monici, M., Pratesi, R., Bernabei, P.A., Caporale, R., Ferrini, P.R., Croce, A.C., Balzarini, P., Bottiroli, G., 1995. Natural fluorescence of white blood cells: spectroscopic and imaging study. J. Photochem. Photobiol. B: Biol. 30(1), 29-37.
Nakai, Y., Anai, S., Onishi, S., Masaomi, K., Tatsumi, Y., Miyake, M., Chihara, Y., Tanaka, N., Hirao, Y., Fujimoto, K., 2015. Protoporphyrin IX induced by 5-aminolevulinic acid in bladder cancer cells in voided urine can be extracorporeally quantified using a spectrophotometer. Photodiagnosis Photodyn Ther 12(2), 282-288.
Nakai, Y., Ozawa, T., Mizuno, F., Onishi, S., Owari, T., Hori, S., Morizawa, Y., Tatsumi, Y., Miyake, M., Tanaka, N., Tsuruta, D., Fujimoto, K., 2017. Spectrophotometric photodynamic detection involving extracorporeal treatment with hexaminolevulinate for bladder cancer cells in voided urine. J. Cancer Res. Clin. Oncol. 143(11), 2309-2316.
Ostrikov, K., Michl, T., MacGregor, M., Vasilev, K., 2019. Bladder Cancer Cell Capture: Elucidating the Effect of Sample Storage Conditions on Capturing Bladder Cancer Cells via Surface Immobilized EpCAM Antibody. ACS Applied Bio Materials 2(9), 3730-3736.
Patriarca, C., Colombo, P., Pio Taronna, A., Wesseling, J., Franchi, G., Guddo, F., Naspro, R., Macchi, R.M., Giunta, P., Di Pasquale, M., Parente, M., Arizzi, C., Roncalli, M., Campo, B., 2009. Cell discohesion and multifocality of carcinoma in situ of the bladder: new insight from the adhesion molecule profile (e-cadherin, Ep-CAM, and MUC1). Int. J. Surg. Pathol. 17(2), 99-106.
Phillips, K., Velasco, C., Li, J., Kolatkar, A., Luttgen, M., Bethel, K., Duggan, B., Kuhn, P., McCarty, O., 2012. Optical Quantification of Cellular Mass, Volume, and Density of Circulating Tumor Cells Identified in an Ovarian Cancer Patient. Front. Oncol. 2(72).
Planz, B., Jochims, E., Deix, T., Caspers, H.P., Jakse, G., Boecking, A., 2005. The role of urinary cytology for detection of bladder cancer. European Journal of Surgical Oncology (EJSO) 31(3), 304-308.
Ramiasa, M.N., Cavallaro, A.A., Mierczynska, A., Christo, S.N., Gleadle, J.M., Hayball, J.D., Vasilev, K., 2015. Plasma polymerised polyoxazoline thin films for biomedical applications. Chem. Commun. 51(20), 4279-4282.
Schmidbauer, J., Witjes, F., Schmeller, N., Donat, R., Susani, M., Marberger, M., Group, H.P.S., 2004. Improved detection of urothelial carcinoma in situ with hexaminolevulinate fluorescence cystoscopy. The Journal of urology 171(1), 135-138.
Shashni, B., Ariyasu, S., Takeda, R., Suzuki, T., Shiina, S., Akimoto, K., Maeda, T., Aikawa, N., Abe, R., Osaki, T., Itoh, N., Aoki, S., 2018. Size-Based Differentiation of Cancer and Normal Cells by a Particle Size Analyzer Assisted by a Cell-Recognition PC Software. Biol. Pharm. Bull. 41(4), 487-503.
Shaw Bagnall, J., Byun, S., Begum, S., Miyamoto, D.T., Hecht, V.C., Maheswaran, S., Stott, S.L., Toner, M., Hynes, R.O., Manalis, S.R., 2015. Deformability of Tumor Cells versus Blood Cells. Sci. Rep. 5(1), 18542.
Shen, C., Sun, Z., Chen, D., Su, X., Jiang, J., Li, G., Lin, B., Yan, J., 2015. Developing urinary metabolomic signatures as early bladder cancer diagnostic markers. Omics : a journal of integrative biology 19(1), 1-11.

Shirazi, H.S., Chan, K.M., Rouget, J., Ostrikov, K., McNicholas, K., Li, J., Butler, L., Gleadle, J.M., Vasilev, K., MacGregor, M., 2020. Plasma enabled devices for the selective capture and photodynamic identification of prostate cancer cells. Biointerphases 15(3), 031002.
Sievert, K.D., Amend, B., Nagele, U., Schilling, D., Bedke, J., Horstmann, M., Hennenlotter, J., Kruck, S., Stenzl, A., 2009. Economic aspects of bladder cancer: what are the benefits and costs? World J. Urol. 27(3), 295-300.
Tan, W.S., Tan, W.P., Tan, M.-Y., Khetrapal, P., Dong, L., deWinter, P., Feber, A., Kelly, J.D., 2018. Novel urinary biomarkers for the detection of bladder cancer: A systematic review. Cancer Treat. Rev. 69, 39-52.
Vasilev, K., MacGregor, M., Gleadle, J., Li, J., 2017. DEVICES AND METHODS FOR DETECTION AND CAPTURE OF BIOLOGICAL ENTITIES IN NON-BLOOD BODY FLUIDS. Australia.
Vasilev, K., Ramiasa, M., Cavallaro, A., 2015. Plasma Polymerised Polyoxazolines and uses thereof. Australia.
Vona, G., Sabile, A., Louha, M., Sitruk, V., Romana, S., Schütze, K., Capron, F., Franco, D., Pazzagli, M., Vekemans, M., Lacour, B., Bréchot, C., Paterlini-Bréchot, P., 2000. Isolation by Size of Epithelial Tumor Cells: A New Method for the Immunomorphological and Molecular Characterization of Circulating Tumor Cells. The American Journal of Pathology 156(1), 57-63.
Witjes, J.A., Douglass, J., 2007. The role of hexaminolevulinate fluorescence cystoscopy in bladder cancer. Nat. Clin. Pract. Urol. 4(10), 542-549.
Wizenty, J., Ashraf, M.I., Rohwer, N., Stockmann, M., Weiss, S., Biebl, M., Pratschke, J., Aigner, F., Wuensch, T., 2018. Autofluorescence: A potential pitfall in immunofluorescence-based inflammation grading. J. Immunol. Methods 456, 28-37.
Yafi, F.A., Brimo, F., Auger, M., Aprikian, A., Tanguay, S., Kassouf, W., 2014. Is the performance of urinary cytology as high as reported historically? A contemporary analysis in the detection and surveillance of bladder cancer. Urologic Oncology: Seminars and Original Investigations 32(1), 27.e21-27.e26.
Yafi, F.A., Brimo, F., Steinberg, J., Aprikian, A.G., Tanguay, S., Kassouf, W., 2015. Prospective analysis of sensitivity and specificity of urinary cytology and other urinary biomarkers for bladder cancer. Urol. Oncol. 33(2), 66.e25-31.
Zanini, S., Zoia, L., Dell'Orto, E.C., Natalello, A., Villa, A.M., Pergola, R.D., Riccardi, C., 2016. Plasma polymerized 2-ethyl-2-oxazoline: Chemical characterization and study of the reactivity towards different chemical groups. Mater. Des. 108, 791-800.
Zhe, X.N., Cher, M.L., Bonfil, R.D., 2011. Circulating tumor cells: finding the needle in the haystack. Am. J. Cancer Res. 1(6), 740-751.
Zink, D., Fischer, A.H., Nickerson, J.A., 2004. Nuclear structure in cancer cells. Nature Reviews Cancer 4(9), 677-687.

Insert Table of Contents artwork here

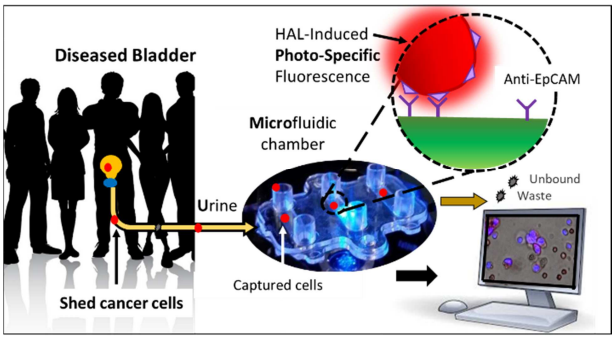

Highlights

- HAL-induced PpIX fluorescence was significantly higher in cancer cell lines than in healthy fibroblast and epithelial cells.
- The technology achieved non-invasive detection of bladder cancer from non-processed urine samples.
- Combining anti-EpCAM immunocapture with HAL-induced fluorescent detection, the technology achieved 100% sensitivity and 80% specificity in the validation cohort.

Declaration of interests

☒ The authors declare that they have no known competing financial interests or personal relationships that could have appeared to influence the work reported in this paper.

☐The authors declare the following financial interests/personal relationships which may be considered as potential competing interests: